

Northward shift of boreal tree cover confirmed by satellite record

Authors

Min Feng^{1,2}; Joseph O. Sexton¹; Panshi Wang¹; Paul M. Montesano^{3,4}; Leonardo Calle⁵; Nuno Carvalhais^{6,7}; Benjamin Poulter^{8,9}; Matthew J. Macander¹⁰; Michael A. Wulder¹¹; Margaret Wooten^{3,12}; William Wagner^{3,12}; Akiko Elders¹³; Saurabh Channan¹; Christopher S.R. Neigh^{3,12}

Affiliations

¹ terraPulse, Inc., North Potomac, Maryland, USA.

² Institute of Tibetan Plateau Research, Chinese Academy of Sciences; Beijing, China.

³ NASA Goddard Spaceflight Center; Greenbelt, Maryland, USA.

⁴ ADNET Systems, Inc.; Bethesda, Maryland, USA.

⁵ calleEcology, Inc., Missoula, MT, USA.

⁶ Max Planck Institute for Biogeochemistry, Jena, Germany.

⁷ Departamento de Ciências e Engenharia do Ambiente, DCEA, Faculdade de Ciências e Tecnologia, FCT, Universidade Nova de Lisboa, Caparica, Portugal.

⁸ Spark Climate Solutions, San Francisco, California, USA.

⁹ Department of Geographical Sciences, University of Maryland, College Park, Maryland, USA.

¹⁰ ABR, Inc.—Environmental Research & Services, Fairbanks, Alaska, USA.

¹¹ Canadian Forest Service (Pacific Forestry Centre), Natural Resources Canada, 506 West Burnside Road, Victoria, British Columbia, Canada.

¹² Science Systems Applications, Inc., Lanham, Maryland, USA.

¹³ Morgan State University, Baltimore, Maryland, USA.

Correspondence to: Min Feng (mfeng@terrapulse.com), Joseph O. Sexton (sexton@terrapulse.com)

28 **Abstract.** The boreal forest has experienced the fastest warming of any forested biome in recent decades. While
29 vegetation–climate models predict a northward migration of boreal tree cover, the long-term studies required to test
30 the hypothesis have been confined to regional analyses, general indices of vegetation productivity, and data calibrated
31 to other ecoregions. Here we report a comprehensive test of the magnitude, direction, and significance of changes in
32 the distribution of the boreal forest based on the longest and highest-resolution time-series of calibrated satellite maps
33 of tree cover to date. From 1985 to 2020, boreal tree cover expanded by 0.844 million km², a 12% relative increase
34 since 1985, and shifted northward by 0.29° mean and 0.43° median latitude. Gains were concentrated between 64°–
35 68°N and exceeded losses at southern margins, despite stable disturbance rates across most latitudes. Forest age
36 distributions reveal that young stands ([up to ≤36 years](#)) now comprise 15.4% of forest area and hold 1.1–5.9 Pg of
37 aboveground biomass carbon, with the potential to sequester an additional 2.3–3.8 Pg C if allowed to mature. These
38 findings confirm the northward advance of the boreal forest and implicate the future importance of the region’s
39 greening to the global carbon budget.

40

41 **1 Introduction**

42 The boreal biome is Earth’s most expansive and ecologically intact forest. The region contains 38 ± 3.1 Pg [Carbon](#)
43 [\(C\)](#) of above-ground biomass (Neigh et al., 2013) and is underlain by 1672 Pg C, summing to total biomass rivaling
44 the tropics and half of global soil C (Gauthier et al., 2015). Its forested area comprises a third of the global total and
45 accounts for 20.8% of the total forest carbon (C) sink (Pan et al., 2011; [Pan et al., 2024](#)). Boreal tree cover also controls
46 the reflective and thermal balance of solar radiation of the high northern latitudes, posing a positive feedback
47 mechanism for greenhouse atmospheric warming (Betts, 2000; Bonan, 2008; Chen et al., 2018; Randerson et al.,
48 2006).

49 The boreal region has experienced the fastest climatological warming of any forest biome, with annual
50 surface temperatures increasing [more than](#) 1.4° C over the past century (IPCC, 2014; [IPCC, 2023](#)). Boreal forest
51 dynamics are highly correlated to climate (Elmendorf et al., 2012; Holtmeier and Broll, 2005; Vége and St-Onge,
52 2009), and increases in vegetation productivity have been observed across the northern high latitudes (Berner and
53 Goetz, 2022). However, regional increases in the frequency and severity of windthrow, fire, insect, and disease events
54 have also been reported (Gauthier et al., 2015; Walker et al., 2019), and a recent analysis by Rotbarth et al. (2023)
55 suggests that southern contraction exceeds northern expansion, yielding net shrinkage of the boreal forest.

56 While theory predicts a northward shift of the boreal forest, the global net effects of climate and other factors
57 on the density and distribution of its tree cover remain untested hypotheses at the spatial and temporal scale of Landsat,
58 Earth’s longest-running record of global, high-resolution satellite imagery. Coupled climate-vegetation models predict
59 a net-northward migration of boreal vegetation due to warming (IPCC, 2018; Scheffer et al., 2012), supporting the
60 dominance of growth processes. Multiple studies (Berner and Goetz, 2022; Sulla-Menashe et al., 2018; Zhu et al.,
61 2016; Piao et al., 2020) have reported vegetation “greening” (e.g., Berner and Goetz, 2022) based on spectral indices
62 of plant productivity. However, the ecological effects of trees differ from those of graminoids, shrubs, and other
63 vegetation, and the comparatively low productivity of boreal ecosystems necessitate long-term analyses that have

64 historically been limited to either regional scales or uncalibrated data (Beck et al., 2011; Brice et al., 2020; Taylor et
65 al., 2017; Rotbarth et al., 2023). As a result, the net effect of growth and mortality on the global distribution of boreal
66 tree cover, and the resulting effect on carbon budgets, remain uncertain (Fan et al., 2023).

67 Here we report a global test of the magnitude and direction of boreal-forest change from 1985 to 2020, as
68 observed through historical satellite records of tree cover calibrated to the boreal biome. We calibrated and expanded
69 a global tree cover dataset (Carroll et al. 2011, Sexton et al., 2013) to 224,026 Landsat images estimating tree cover
70 and its changes over the global extent of the boreal forest and adjacent tundra at annual, 30-meter resolution over 36
71 years (Fig. S1)—the most extensive and highest-resolution record of boreal tree cover to date. This pan-boreal time
72 series was then subjected to trend analysis to estimate and map the historical direction, rate, and significance of change
73 across the region, and the resulting estimates of forest age were used to infer impacts on the region’s carbon budget.

74

75 **2 Methods**

76 **2.1 Historical retrieval of tree cover**

77 To improve characterization of boreal forest structure, we calibrated the 250-m resolution, 2000 - 2020 MODIS
78 Vegetation Continuous Fields (VCF) Tree Cover product (MOD44B Collection 6; Carroll et al., 2011) against a
79 region-wide sample of airborne lidar measurements, stratifying by topographic and bioclimatic covariates
80 ([Supplemental Information \(SI\) §2–4](#)). This boreal-specific calibration improved characterization of tree-cover
81 gradients across the boreal region (Fig. S7), increasing accuracy, decreasing uncertainty, and improving the linear
82 correlation of per-pixel fractional tree cover estimates to reference measurements (Fig. S8). Mean absolute error
83 (MAE) decreased to 11.13%, root-mean-squared error (RMSE) decreased to 16.44%, and the coefficient of
84 determination (R^2) of the linear model between estimated and measured data increased to 0.60. ~~Following calibration,~~
85 ~~the calibrated MODIS VCF estimates were downscaled to 30-meter resolution and extended from 1984 to 2020~~
86 ~~following Sexton et al. (2013). The residual bias of the Landsat-based estimates relative to the lidar reference~~
87 ~~measurements was slight (~2%, SI).~~

88 The calibrated MODIS VCF estimates were then downscaled to 30-m resolution and extended to 1984–
89 2020 by applying a machine learning model (gradient-boosted regression tree) to Landsat surface reflectance imagery
90 from sensors [Thematic Mapper \(TM\)](#), [Enhanced Thematic Mapper Plus \(ETM+\)](#), and [Operational Land Imager \(OLI\)](#)
91 (Sexton et al., 2013; SI §5–6). A total of 224,026 Landsat scenes across 2,189 [World Reference System 2 \(WRS-2\)](#)
92 tiles was used to reconstruct annual tree cover estimates, composited to minimize cloud, snow, and phenological noise.
93 For each pixel-year, the median value of valid observations was retained, resulting in a consistent, high-resolution
94 time series of tree cover estimates (Fig. S5–S7). [The residual bias of the Landsat-based estimates relative to the](#)
95 [lidarLiDAR reference measurements was slight \(~2%, SI\).](#)

96

97 **2.2. Tree cover trend analysis**

98 The calibrated, downscaled, and extended tree cover values were then summarized across the region as annual,
99 boreal-wide means and medians to calculate changes over the 36-year study span (Fig. 2). The annual mean and
100 median tree cover were also broken down by latitude to calculate the change rate at each latitudinal degree between

101 47°N to 70°N (Fig. S10). Tree cover estimates for 1984 were excluded from the trend analysis due to the poor spatial
102 coverage in the first operational year of Landsat 5 (Fig. S2), and pixels with less than 30 unobscured annual tree
103 cover observations were excluded to minimize unbalanced representation caused by the lapses in the availability of
104 Landsat images, mainly in central and northeast Siberia (Neigh et al., 2013; Sexton et al., 2013).

105 106 **2.3. Detection of forest change and estimation of age**

107 Following the United Nations Framework Convention on Climate Change (UNFCCC, 2002), forest was defined as
108 tree cover exceeding 30% within each 30-m pixel. The probability of a pixel being forested, $p(F)$, was calculated as
109 the integral of the probability density function of tree cover values exceeding this 30% threshold (SI §11). Using the
110 36-year time series of annual, 30-m resolution estimates of forest probability ($p(F)$), forest changes, i.e., gains and
111 losses, were identified by applying a two-sample z-test in a moving kernel centered on transitions across the 50%
112 threshold of $p(F)$ (Fig. S13).

113 Pixels with multiple statistically significant transitions during the 1985–2020 period were permitted up to
114 three gain or loss events. ~~Disturbances-Forest changes~~ were classified as “incomplete” if more than 7 years of data
115 were missing, and “incomplete” otherwise. Incomplete ~~disturbances-changes~~ were concentrated in areas with sparse
116 Landsat acquisitions prior to 1999, before implementation of systematic global imaging by Landsat 7 (Sexton et al.,
117 2013; Potapov et al., 2012).

118 Forest age was estimated for each year and pixel by subtracting the year of the most recent significant forest gain from
119 the year of interest. Pixels were classified as “new” forests if no forest cover or loss had been observed earlier in the
120 time series within a 150-m radius (five Landsat pixels); otherwise, forests were considered “recovering.” This
121 approach does not capture the initial years of seedling establishment and growth when cover is below this detection
122 threshold. Also, because of the limited Landsat period, areas detected as “new” forest may actually be “recovering”
123 from pre-1985 disturbances. Accuracy of change detection and age estimation was assessed against a reference sample
124 of 2,404 visually interpreted points distributed across the boreal biome (SI Fig. S14 and S15).

125 126 **2.4. Estimation of aboveground biomass**

127 Aboveground biomass carbon (AGB) was estimated as a function of forest stand age using a linear growth model
128 (Cook-Patton et al., 2020; Fig. S16), with intercept ($\mu = -35.7$, $\sigma = 12.6$) and slope coefficients ($\mu = 23.2$, $\sigma = 3.2$)
129 incorporating parametric uncertainty. Because ages of forests older than the 36-year time-series could not be directly
130 observed, we assumed three scenarios of stand age to bracket carbon stock estimates in these undated stands: the
131 absolute minimum possible age (36 years) yielding 19.1–58.4 Pg C, and typical ages for mature and old-growth
132 stands in boreal ecosystems, i.e., 100 years yielding 35.8–80.5 Pg C, and 300 years yielding 42.4–89.2 Pg C.

133 These scenarios define the plausible envelope of legacy biomass in mature forest. However, estimates reflected
134 structural biomass only and did not account for potential effects of changes in soil moisture or variation in respiration
135 rates. To contextualize the biomass sink relative to climate-driven emissions, we also evaluated the trend in regional
136 surface air temperature using the Climate Research Unit (CRU) dataset and the European Centre for Medium-Range
137 Weather Forecasts (ECMWF) ERA-Interim reanalysis~~two reanalysis products~~. Both records indicated significant

138 warming over the study period, with trends of $0.038^{\circ}\text{C yr}^{-1}$ ($r = 0.69$, $p < 1 \times 10^{-5}$) and $0.035^{\circ}\text{C yr}^{-1}$ ($r = 0.73$, $p <$
139 1×10^{-6}) respectively (Fig. S17).

140 3 Results

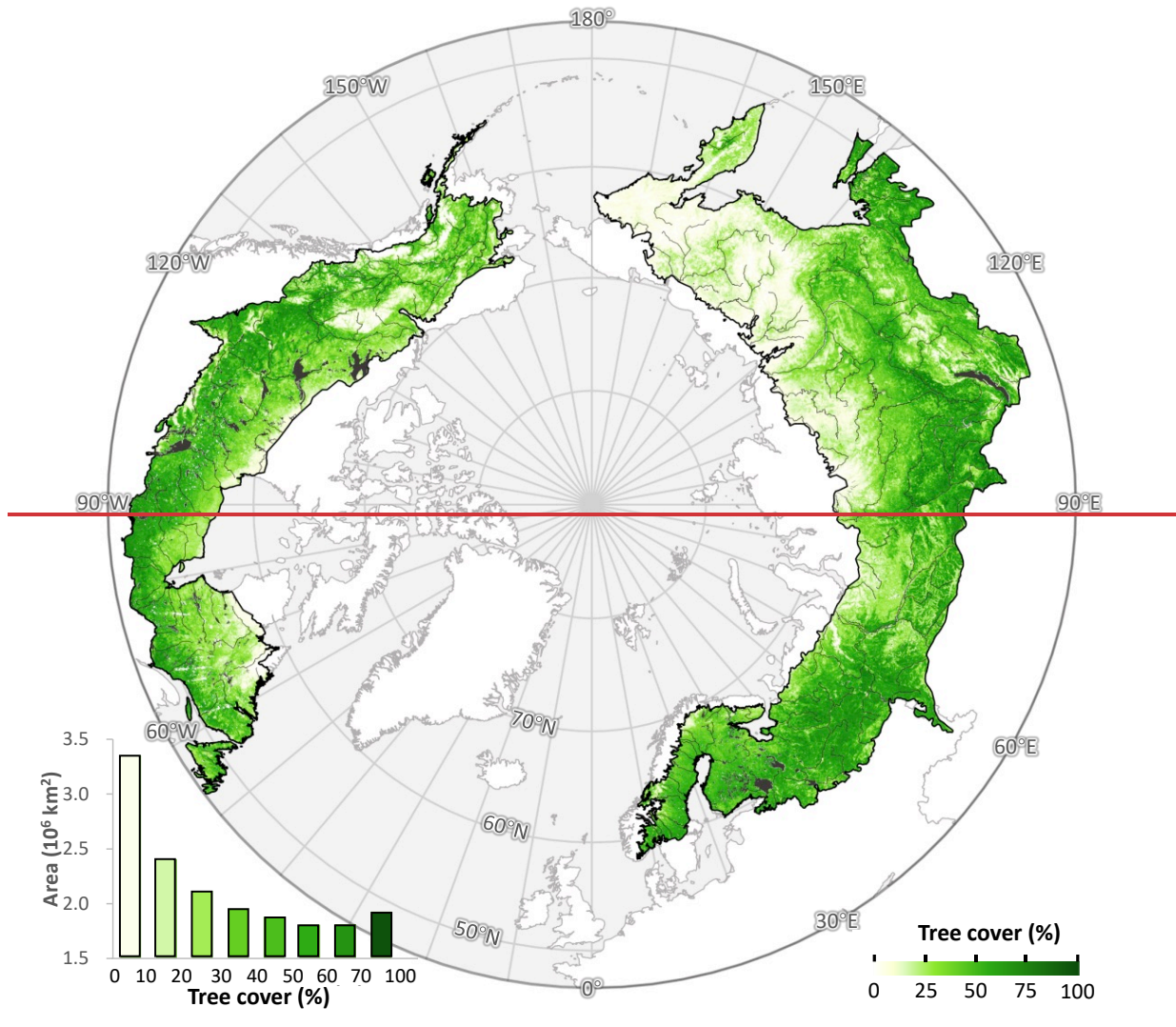
141 3.1. Distribution of boreal tree cover

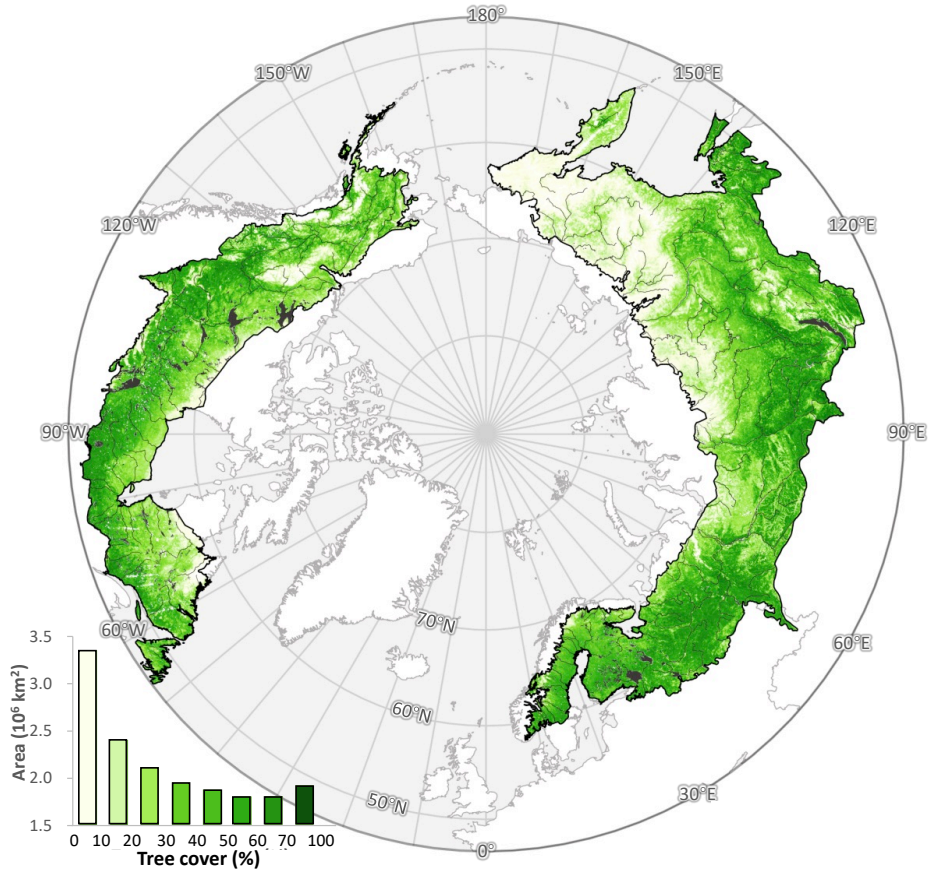
142 Tree cover reaches its highest densities in the southern portion of the boreal biome and decreases progressively
143 northward (Fig. 1). Sparse conifer stands, woodlands, herbaceous vegetation, and unvegetated barrens dominate the
144 transition to Arctic tundra, and tree cover is nearly absent north of 71°N . Due to interspersed tundra, wetlands, and
145 inland water bodies, the most common local (i.e., 30-meter pixel) tree-cover density across the entire boreal forest and
146 taiga-tundra ecotone is below 5%.

147 ~~From 1985 to 2020, boreal tree cover increased by 0.844 million km^2 , a 4.3 percentage point absolute increase~~
148 ~~and a 12% relative increase over its 1985 extent (Fig. 1).~~ Boreal tree cover expanded from 7.153 million km^2 (41.44%
149 of the region) in 1985 to 7.997 million km^2 (46.32%) in 2020, with a linear trend of 0.023 million $\text{km}^2 \text{ yr}^{-1}$ (0.12%
150 yr^{-1} ; percent cover = $0.116 \times \text{year} - 187.6$, $R^2 = 0.99$, $p < 0.001$) (Fig. 1). ~~From 1985 to 2020, the boreal tree cover~~
151 ~~increased by 0.844 million km^2 , a 4.3 percentage point absolute increase and a 12% relative increase over its 1985~~
152 ~~extent.~~ Applying the UNFCCC forest definition of 10–30% tree cover (UNFCCC, 2002; Sexton et al., 2016), the
153 region held between 8.95 and 12.41 million km^2 of forest in 2000 and between 9.41 and 13.26 million km^2 in 2020.

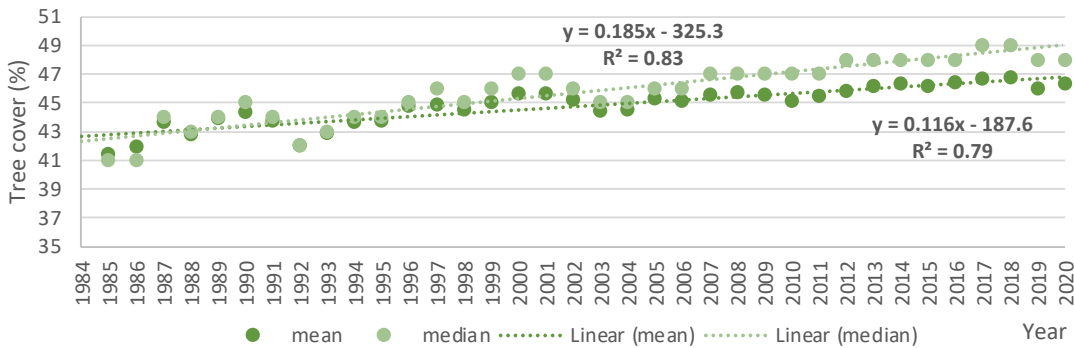
154 The latitudinal distribution of tree cover also shifted northward from 1985 to 2020. The mean latitude of tree
155 cover increased by 0.29° , from 57.37°N in 1985 to 57.66°N in 2020 (mean latitude = $0.0075 \times \text{year} + 42.6$, $R^2 = 0.79$,
156 $p < 0.001$). The median latitude increased more rapidly, by 0.43° (median latitude = $0.0124 \times \text{year} + 32.5$, $R^2 = 0.88$,
157 $p < 0.001$), indicating widespread net expansion across the biome rather than outliers of change at either its northern
158 or southern extremes.

159





161



162

163

164

165

Fig. 1. Distribution of tree cover boreal across boreal and arctic tundra ecoregions in 2020. Estimates from 2020 are shown. Data gaps due to clouds were filled with estimates from earlier years. Ecoregions were defined by Dinerstein et al (2017). The bottom panel shows the increasing density in the overall, pan-boreal density of tree cover from 1985 to 2020.

166

167

3.2. The pace and pattern of boreal forest change

168

169

170

171

Net biome-wide changes were underlain by strong geographic variation (Fig. 2). Net gains from 1985 to 2020 occurred at all latitudes above 53°N, with the strongest increases concentrated between 64° and 68°N. Gains in the northernmost latitudes support the hypothesis of a poleward shift in the northernmost extent of tree cover and are consistent with findings by Montesano et al. (2024), who reported long-term increases in deciduous and mixed forest components in

172 transitional boreal zones. These structural shifts parallel recent evidence that warming-induced species diversification
173 is strongest near the tundra margin as temperate species colonize newly viable habitat (Xi et al., 2024). In contrast,
174 net losses were smaller in magnitude and limited to the southern boreal latitudes (47°–52°N), corroborating recent
175 observations by Rotbarth et al. (2023) ~~(Fig. 3)~~.

176 Our analysis of calibrated, high (30-meter) resolution estimates of tree cover minimized potential for
177 herbaceous growth to obscure tree mortality, for which coarser-resolution, [The Normalized Difference Vegetation](#)
178 [Index \(NDVI\)](#)-based analyses have been criticized (Yan et al., 2024). The pan-boreal expansion of tree cover occurred
179 against relatively stable disturbance rates over the study period (Fig. 3), and observed disturbances influenced regional
180 patterns but did not obscure the biome-wide trend. The annual rate of disturbance increased modestly from 53,546
181 km² yr⁻¹ in 2000 to 60,275 km² yr⁻¹ in 2020, equivalent to a 1.8% yr⁻¹ [linear](#) increase (1,100 km² yr⁻¹), or approximately
182 0.2%–0.4% of the forested area. Locations undisturbed between 1985 and 2020 exhibited net gains across nearly all
183 latitudes, and the latitudinal distribution of disturbance—while varying strongly among years—remained broadly
184 stationary over time. (Fig. S10).

185 In North America, the largest gains were concentrated in the northernmost boreal, where increases in shrubs
186 and grasses have also been reported (McManus et al., 2012). Areas of net loss corresponded to widespread forest
187 disturbances, including wildfire and bark beetle (*Dendroctonus* spp.) outbreaks in British Columbia (Meddens et al.,
188 2012), spruce budworm (*Choristoneura* spp.) in Quebec (Boulanger and Arseneault, 2004), and wildfire across
189 western Canada and interior Alaska (Stocks et al., 2002). Recent shifts in transitional forest structure and composition
190 noted by Montesano et al. (2024) lend further weight to these observations, suggesting a biome-wide response in
191 functional traits, including increased deciduous dominance at the taiga-tundra ecotone. These findings are also
192 partially corroborated by Rotbarth et al. (2023), who also reported tree cover gains in the boreal interior of North
193 America but loss at the southern margins, especially in areas impacted by wildfire and harvest.

194 In Eurasia, hotspots of forest loss included the eastern Russian–Chinese border, agricultural zones south of
195 the Urals, and regions affected by timber harvesting near the Russia–Finland border in the 1990s (Potapov et al.,
196 2012). Logging and fire contributed to localized loss in eastern Russia (Krylov et al., 2014), whereas gains in northern
197 Europe were associated with silvicultural management, afforestation, and fire suppression (Henttonen et al., 2017).
198 Recent analyses confirm extensive regrowth in post-agricultural and permafrost-transitioning landscapes in Russia,
199 where lidar and optical remote sensing reveal increases in regeneration potential, particularly in abandoned or
200 disturbed sites (Neigh et al., 2025).

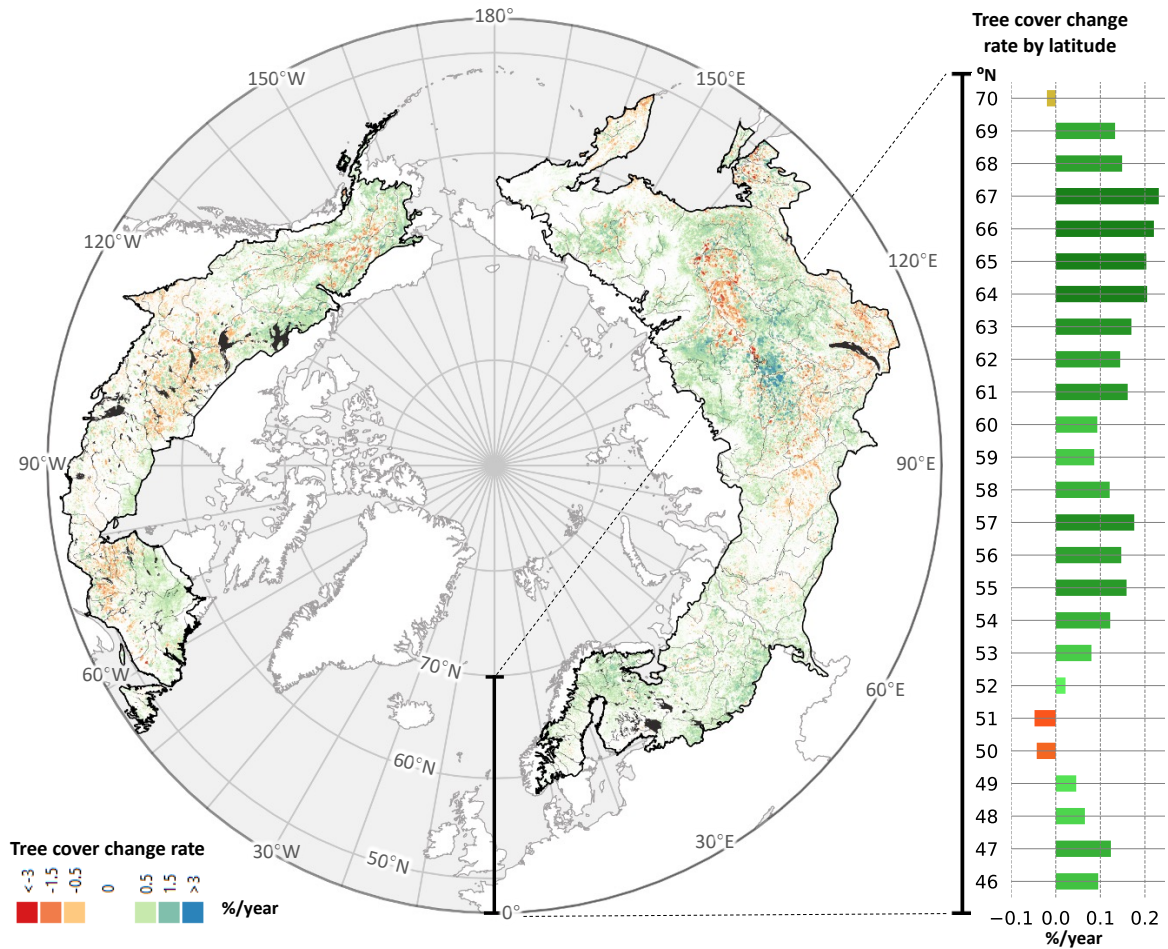
201 In Asia, net gains were observed in areas of post-Soviet agricultural abandonment, as well as in larch forests
202 near the Yakutsk permafrost zone. These trends are consistent with increases in tall shrubs and larch (*Larix* spp.) at
203 the taiga–tundra boundary (Frost and Epstein, 2014). Recovery from wildfires in the 1990s continues in these regions
204 (Kajii et al., 2002), and permafrost thaw has been hypothesized to enhance productivity (Sato et al., 2016).

205 Although we did not attempt to demarcate or detect changes in a discrete tree line, our observations
206 corroborate the boreal advancement hypothesis alongside field measurements of woody vegetation near the northern
207 limits of tree growth and satellite-based studies demarcating the northern tree line (Frost and Epstein, 2014; Rees et
208 al., 2020; Dial et al., 2024; Dial et al., 2022; Rotbarth et al. 2023). While analysis of tree-cover estimates avoided the

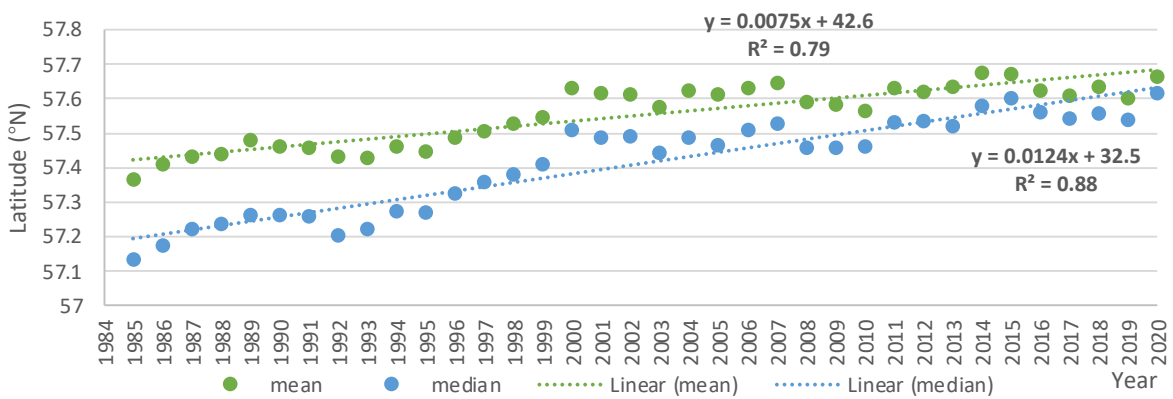
209 potential confusion of changes in trees specifically with general NDVI-based “greening” (Yan et al. 2024), the trend’s
210 geographic variations correspond to general patterns of greening across the biome (Berner and Goetz, 2022; Sulla-
211 Menashe et al., 2018; Zhu et al., 2016; Piao et al., 2020; Guay et al., 2014).

212 Field studies have shown that climate, soil properties, and forest management drive large differences in boreal
213 tree growth rates across the ecotone (Henttonen et al., 2017; Henttonen et al., 2017; Hofgaard et al., 2009). Recent
214 shifts in transitional forest structure and composition noted by Montesano et al. (2024) lend further weight to these
215 observations, suggesting a total biome-wide response in functional traits, including increased deciduous dominance
216 near treeline margins. Xi et al. (2024) further demonstrate that increasing diversity near the forest–tundra boundary is
217 associated with moderate climatic warming, although they caution that the gains are vulnerable to reversal under
218 extremes such as drought and heatwaves. Changes in species composition remain a focal point of research (Xi et al.,
219 2024; Mekonnen et al., 2019; Massey et al., 2023; Mack et al., 2021; Liski et al., 2003), while still remaining to be
220 explored are the differentiation of climate and soil effects at the global scale and the discrimination of tree cover
221 expansion due to the establishment and growth of new seedlings versus the widening of existing tree crowns.

222



223



224

225

226

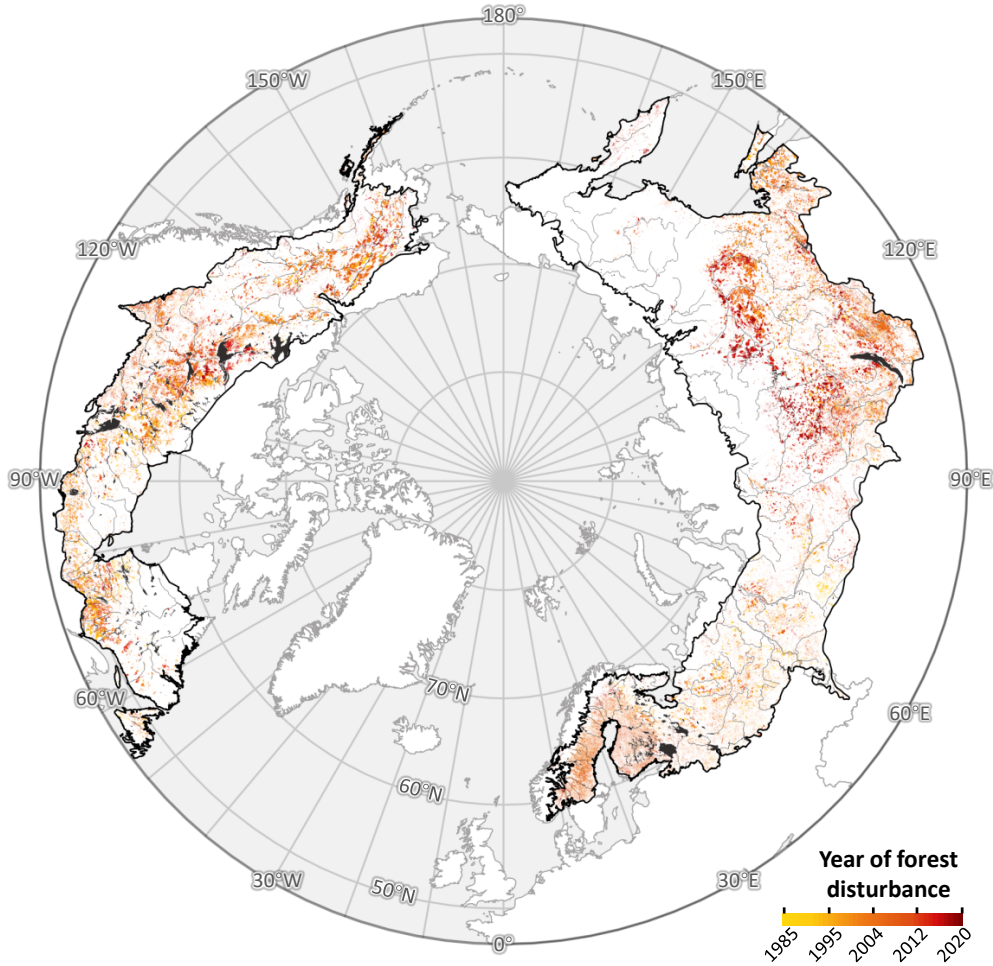
227

228

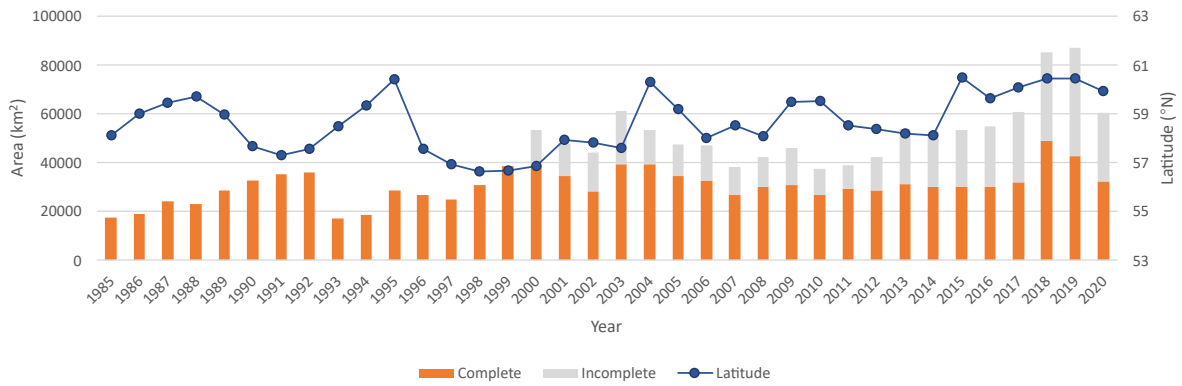
229

Fig. 2. Spatial and temporal distribution of boreal tree cover change from 1985 to 2020. Map: significant net gains (green-blue) and losses (orange-red) of tree cover over the boreal biome. Bar chart (top-right): linear regression slope of tree cover over time, stratified by latitude. Time series (bottom): northward migration of the distribution of mean and median latitude of tree cover. Every 30-m resolution pixel included in the analysis had >30 unobscured annual tree cover estimates between 1985 and 2020.

230



231



232

233 **Fig. 3. Total area and median latitude of boreal stand-clearing disturbances from 1985 to 2020. Trends are plotted for the**
 234 **portion of the boreal area where the satellite image is complete from 1984 to 2019 (“complete”) and from all locations,**
 235 **including where the satellite record is incomplete (“incomplete”) (Supplemental Information).**

236

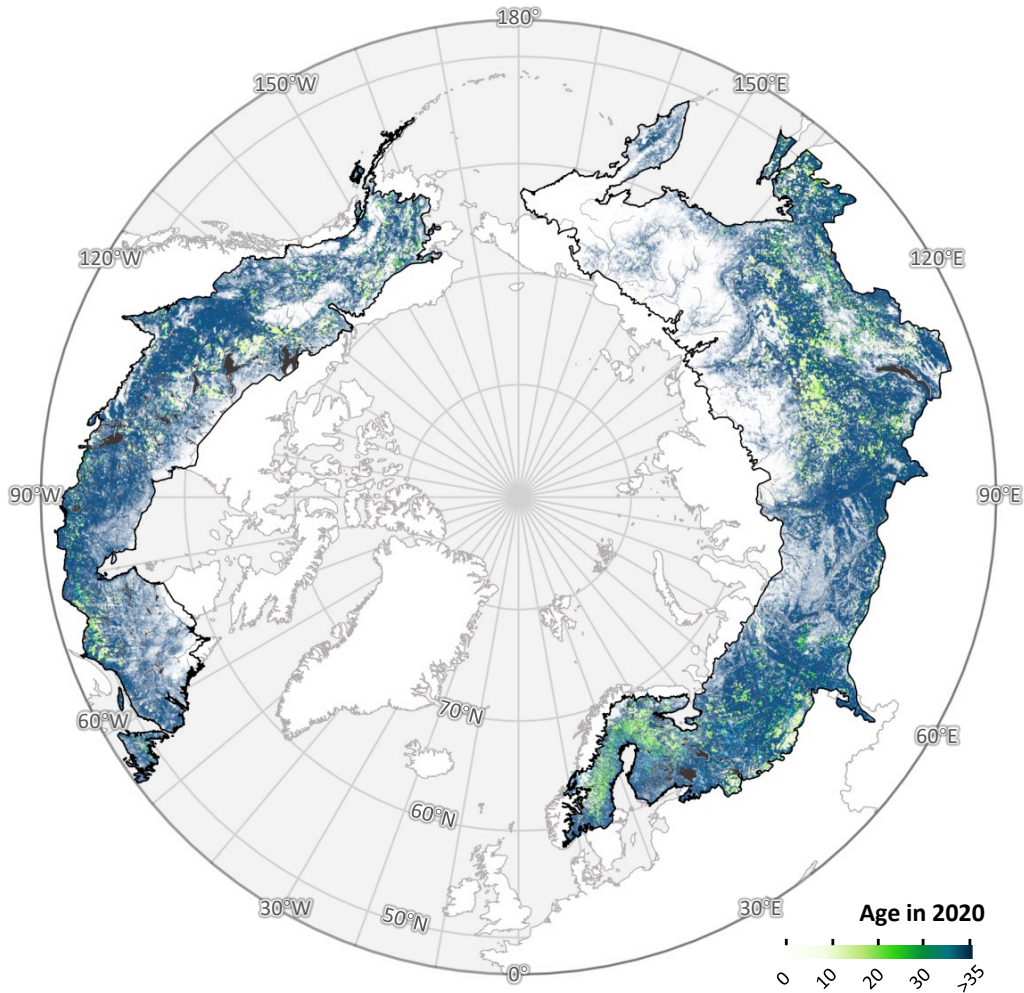
237 **3.3. The distribution of boreal forest age**

238 Most of the boreal forest—8.19 million km², or 47.5% of the region—is older than can be directly measured from the
239 satellite record (Fig. 4). Tree cover in these older stands was already established by the beginning of the Landsat
240 observation period in 1985, and the slow rates of biomass accumulation in boreal ecosystems further complicate the
241 detection of recent forest establishment (SI-Fig. S15). However, the age of younger stands can be estimated by
242 subtracting the year of first detected forest cover from 2020. The forest age estimator showed a root mean square error
243 (RMSE) of 17.46 years and a mean bias of -3.27 years relative to reference data. These errors indicate that while the
244 age maps capture broad spatial patterns and distributions, they should not be interpreted as precise pixel-level
245 predictions. Instead, the results are most reliable when aggregated to regional or biome scales, where random errors
246 are reduced.

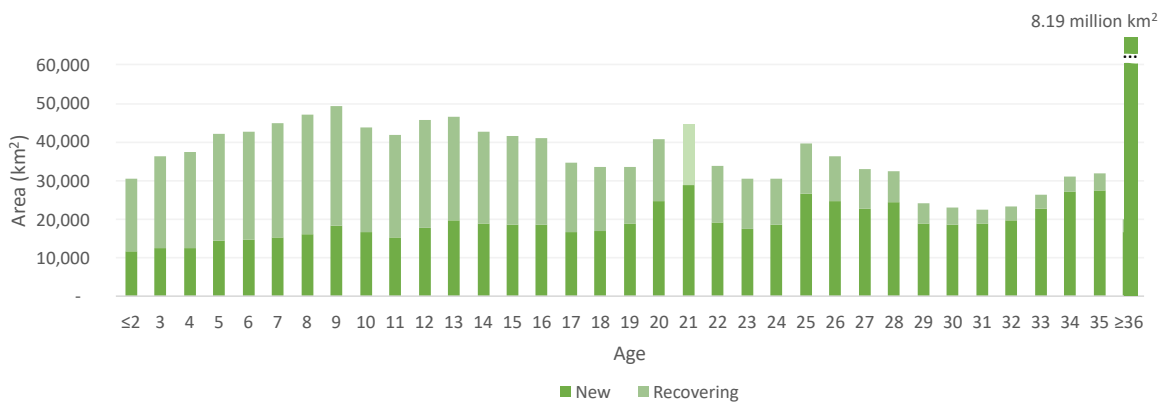
247 Of the forested area present in 1985, 0.5 million km²—representing 5.29% of standing forests—was disturbed
248 during the study period and recovered to forest by 2020. Recovering forests, combined with “new” forests gained
249 during the Landsat era, produced a weak modal age class centered between 9 and 21 years, with a notable lapse in the
250 youngest age classes. These young forests were concentrated in regions of intensive silviculture, including industrial
251 plantations in Scandinavia (Henttonen et al., 2017; Liski et al., 2003; Ågren et al., 2008), and in areas recovering from
252 wildfire. The latter trend is corroborated by reports of increasing burn frequency and extent in Siberia since the late
253 20th century (Kharuk et al., 2021), which has driven a rising proportion of recovering forest younger than 20 years.

254

255



256



257

258 **Fig. 4. Spatial distribution of stand age (top) across the boreal ecoregion and frequency distribution of boreal stand age in**
 259 **2020 (bottom). Forest age-class distribution is defined as years since establishment of pixels identified as forest in 2020.**
 260 **“New” forests were identified as pixels with forest cover following a gain but no prior forest cover or loss earlier in the time**
 261 **series within a 150-m radius (5 pixels) over the observable period (1984 – 2020); “recovering” forests were identified as**
 262 **pixels with forest cover following a gain where a forest loss had been observed previously in the series (Supplemental**
 263 **Information).**

264

265 4 Discussion

266 The expansion and redistribution of boreal tree cover documented in this study has direct implications for the region's
267 role in the global carbon cycle. Between 1985 and 2020, boreal tree cover increased by 0.844 million km² and shifted
268 northward by over 0.4° in median latitude, with gains concentrated at the biome's northern margin and net expansion
269 observed across most latitudes. These changes are not only spatially extensive but demographically consequential:
270 they reflect a growing fraction of young forests with distinct structural and functional attributes that position them as
271 dynamic agents of carbon sequestration. Understanding the contribution of these forests to current and future carbon
272 stocks is essential for anticipating the net climate feedbacks emerging from boreal ecosystems.

273
274 Recent models relating forest age to biomass dynamics suggest that shifting age structure will substantially
275 influence the boreal region's contribution to the global carbon budget in the coming decades. Young forests already
276 contribute significantly to the region's carbon sink (Pan et al., 2011). Forest age estimates carry substantial uncertainty
277 (RMSE ≈ 17 years), limiting their precision at the pixel scale. They remain useful for identifying large-scale patterns
278 and average age structures, but future work will be required to reduce error and quantify regional biases. Forests with
279 known stand ages (≤(less than 36 years since disturbance) hold between 1.1 and 5.9 Pg C in aboveground biomass,
280 based on global growth models (Cook-Patton et al., 2020). The ages of forests where no disturbance was observed
281 during the satellite era remain unknown, but plausible aboveground carbon stocks in these older stands can be
282 bracketed between a low-end scenario assuming 36 years of age (19.1–58.4 Pg C) and a high-end scenario assuming
283 300 years (42.4–89.2 Pg C). Based on these estimates, forests younger than ≤36 years of age comprise 1.35–14.20%
284 of the total boreal aboveground biomass carbon stock—consistent with their 15.4% share of total forest area. Including
285 belowground biomass would raise these values by approximately 25%, based on a mean global root:shoot ratio of
286 0.25 (Huang et al., 2021).

287 If allowed to mature without further disturbance, these young forests could sequester an additional 2.3–3.8
288 Pg C in aboveground biomass. Forests newly established during the observation period contribute between 0.8 and
289 3.5 Pg C today, exceeding the 0.3–2.4 Pg C held in forests recovering from recorded disturbances. Over the next 36
290 years, new forests represent a potential additional aboveground sink of 1.3–2.0 Pg C (0.036–0.18 Pg C yr⁻¹), compared
291 to 1.0–1.8 Pg C (0.028–0.05 Pg C yr⁻¹) from recovering forests. This distinction reflects both the greater area occupied
292 by new forests (7.6% vs. 6.7%) and their older mean stand age. These findings support recent observations by Neigh
293 et al. (2025), who reported a disproportionately large contribution of young, regrowing stands to carbon storage in the
294 Russian boreal.

295 The additional carbon in new forests could help offset warming-induced increases in boreal ecosystem
296 respiration, which have been estimated between 5 and 28 Pg C from 1985 to 2020 (SI-Fig. S16). Both climate warming
297 and carbon dioxide (CO₂) fertilization are expected to enhance productivity (Norby and Zak, 2011), and the spatial
298 pattern of observed tree-cover growth aligns with model predictions of increased seasonal CO₂ exchange above 40°N
299 (Forkel et al., 2016). However, several mechanisms may limit this offset. First, temperature sensitivity of respiration
300 can itself be temperature-dependent (Koven et al., 2017). Second, carbon accumulation rates decline with forest age
301 (Odum, 1969). Third, thawing of permafrost can release substantial legacy carbon stocks (Schuur et al., 2015). Fourth,

302 increases in fire and harvest activity may reverse regional gains in biomass (Gauthier et al., 2015; Kharuk et al., 2021).
303 Compositional and functional transitions may also alter sink dynamics (Montesano et al., 2024; Xi et al., 2024).

304 The long-term persistence of tree-cover expansion depends not only on productivity, but also on the capacity
305 of boreal soils to support woody vegetation. It remains uncertain whether boreal soils—especially under changing
306 permafrost regimes—can structurally sustain expanded forest cover (Koven, 2013). Additional uncertainty stems from
307 the rising role of anthropogenic fire in some parts of the boreal zone (Doerr and Santín, 2016; Mollicone et al., 2006).
308 Our biomass estimates are derived from models for natural forests and do not account for differences between managed
309 and unmanaged systems (Kuuluvainen and Gauthier, 2018) or for anticipated changes in fire regimes.

310 While expansion of tree cover may imply increased carbon storage, nonlinear biodiversity responses to
311 warming complicate projections. Enhanced taxonomic and functional diversity may improve ecological resilience (Xi
312 et al., 2024), but these benefits are constrained by the growing frequency of climatic extremes. Moreover, biodiversity-
313 related feedbacks on carbon balance remain difficult to predict under scenarios of increasing disturbance. Ultimately,
314 all of these processes—forest growth, mortality, disturbance, and compositional change—are already underway across
315 the boreal biome. Quantifying the balance of autotrophic and heterotrophic carbon fluxes remains critical to
316 understanding and managing the global climate system.

317 While our calibration was stratified across ecological and topographic gradients to minimize overfitting, more
318 stringent tests could be obtained by withholding subsets of the reference data (e.g., complete LVIS flightlines or high-
319 resolution imagery tiles) within specific ecozones and revalidating predictions at those sites. Such “leave-tile-out”
320 cross-validation would provide a direct assessment of model transferability at biome boundaries, including ecotones.
321 A limitation is the absence of temporally repeated reference data, which prevents direct assessment of stability (bias
322 drift). Our calibration and annual compositing reduce some risks, but nonstationary, unaccounted-for sensor
323 differences, phenological shifts, and atmospheric noise remain possible contributors to temporal bias.

324 The accuracy of the reference datasets themselves warrants consideration. Montesano et al. (2023) showed
325 that LVIS canopy heights agree closely with NASA G-LiHT airborne LiDAR, with coefficients of determination (R^2)
326 up to 0.87 and root mean square errors of approximately 1–2 m depending on canopy cover and temporal offset. G-
327 LiHT, with its high point density and small footprint, is widely regarded as a reference standard, though its own
328 absolute error was not quantified in that study. For high-resolution optical reference data (QuickBird imagery, Google
329 Earth interpretations), prior work (Montesano et al. 2009, 2016) demonstrated their utility in validating coarse-
330 resolution products but also did not report independent accuracy or inter-observer precision. These limitations
331 highlight the need for future work to establish formal error budgets for reference datasets, while affirming that they
332 provide the best available benchmarks for tree cover calibration and validation.

333 **Summary and Conclusions**

334 This pan-boreal assessment provides the strongest empirical confirmation to date of a northward shift in boreal tree
335 cover, long hypothesized by climate–vegetation models. By retrieving the longest, highest-resolution, and most
336 spatially complete record of calibrated boreal tree cover available, we applied machine learning to the [Landsat 4, 5, 7,](#)
337 [and 8 surface reflectance archives](#)~~Landsat archive~~ to reconstruct annual, 30-m maps of forest change from 1985 to

338 2020. Time-series analysis of 1.9×10^8 pixels revealed widespread increases in tree-cover density and a poleward shift
339 in forest distribution, occurring despite relatively stable disturbance rates across the biome.

340 Although the net trends are globally significant, they mask substantial geographic and temporal
341 heterogeneity, as well as complexity in the ecological processes underlying forest change. These results underscore
342 the need for high-resolution, disturbance-aware metrics to supplement NDVI-based assessments, particularly in
343 climatically sensitive boreal transition zones (Yan et al., 2024). A more complete understanding of boreal forest
344 dynamics will require integration of satellite time series with field-based measurements of canopy structure and the
345 environmental drivers of growth, mortality, and species turnover. Moreover, translating the resulting information into
346 action to forestall and adapt to climate change will require effective communication across scientific, government,
347 and commercial domains of human activity.

348 **Acknowledgments**

349 This research was supported by the NASA Carbon Cycle Science Program (NNH16ZDA001N-CARBON), National
350 Science Foundation Arctic System Science Program (1604105), and NASA ABoVE (80NSSC19M0112). Satellite
351 image processing was performed by terraPulse, Inc. on Amazon Web Services (AWS). Reference data for calibration
352 and validation was produced on the NASA Goddard Spaceflight Center ADAPT and HEC clusters. Aaron Wells
353 (ABR, Inc.), Celio De Sousa (NASA Goddard Space Flight Center, URSA, Inc.), and Jaime Nickeson (NASA
354 Goddard Space Flight Center, SSAI, Inc.) contributed reference observations of forest cover and disturbance.
355 Resources supporting this work were provided by the NASA High-End Computing Program through the NASA Center
356 for Climate Simulation at Goddard Space Flight Center.

357 **Author Contributions**

358 MF and JS designed and developed the tree-cover and forest-change algorithms. PM, PW, and MM conducted the
359 validation and calibration. CN and PM co-edited the manuscript, CN secured research funding to conduct the
360 study. BP commented on the final manuscript. NC and LC conducted the carbon impact analysis. NC conducted the
361 ecosystem respiration analysis. SC developed the platform on AWS. MW, WW, and AE interpreted the validation
362 dataset. JS conceived the study and compiled the manuscript with contributions from all coauthors.

364 **References**

365 Ågren, G. I., Hyvönen, R., and Nilsson, T.: Are Swedish forest soils sinks or sources for CO₂—model analyses based
366 on forest inventory data, *Biogeochemistry*, 89, 139–149, <https://doi.org/10.1007/s10533-007-9121-0>, 2008.

367 Baltzer, J. L., Alexander, H. D., Greaves, H. E., Boulanger, Y., Gauthier, S., Fuller, M. M., and Beck, P. S. A.:
368 Increasing fire and the decline of fire-adapted black spruce in the boreal forest, *Proc. Natl. Acad. Sci. USA*, 118,
369 e2024872118, <https://doi.org/10.1073/pnas.2024872118>, 2021.

370 Beck, P. S. A., Juday, G. P., Alix, C., Barber, V. A., Winslow, S. E., Sousa, E. E., Heiser, P., Herriges, J. D., and
371 Goetz, S. J.: Changes in forest productivity across Alaska consistent with biome shift, *Ecol. Lett.*, 14, 373–379,
372 <https://doi.org/10.1111/j.1461-0248.2011.01598.x>, 2011.

373 Berner, L. T., and Goetz, S. J.: Satellite observations document trends consistent with a boreal forest biome shift,
374 *Glob. Change Biol.*, 28, 3275–3292, <https://doi.org/10.1111/gcb.16100>, 2022.

375 Betts, R. A.: Offset of the potential carbon sink from boreal forestation by decreases in surface albedo, *Nature*, 408,
376 187–190, <https://doi.org/10.1038/35041545>, 2000.

377 Bonan, G. B.: Forests and climate change: Forcings, feedbacks, and the climate benefits of forests, *Science*, 320,
378 1444–1449, <https://doi.org/10.1126/science.1155121>, 2008.

379 Boulanger, Y., and Arseneault, D.: Spruce budworm outbreaks in eastern Quebec over the last 450 years, *Can. J. For.*
380 *Res.*, 34, 1035–1043, <https://doi.org/10.1139/x03-269>, 2004.

381 Brice, M., Boucher, Y., Girardin, M. P., Marchand, W., Tremblay, J.-P., and Krause, C.: Moderate disturbances
382 accelerate forest transition dynamics under climate change in the temperate–boreal ecotone of eastern North America,
383 *Glob. Change Biol.*, 26, 4418–4435, <https://doi.org/10.1111/gcb.15115>, 2020.

384 Bunn, A. G., and Goetz, S. J.: Trends in satellite-observed circumpolar photosynthetic activity from 1982 to 2003:
385 The influence of seasonality, cover type, and vegetation density, *Earth Interact.*, 10, 1–19,
386 <https://doi.org/10.1175/EI190.1>, 2006.

387 Carroll, M., DiMiceli, C., Sohlberg, R., Huang, C., and Hansen, M. C.: MODIS Vegetative Cover Conversion and
388 Vegetation Continuous Fields, in: *Land Remote Sensing and Global Environmental Change: NASA’s Earth Observing*
389 *System and the Science of ASTER and MODIS*, edited by: Ramachandran, B., Justice, C. O., and Abrams, M. J., 725–
390 745, Springer, New York, NY, https://doi.org/10.1007/978-1-4419-6749-7_32, 2011.

391 Chen, D., Loboda, T. V., He, T., Zhang, Y., and Liang, S.: Strong cooling induced by stand-replacing fires through
392 albedo in Siberian larch forests, *Sci. Rep.*, 8, 4821, <https://doi.org/10.1038/s41598-018-23050-9>, 2018.

393 Ciais, P., Yao, Y., Gasser, T., Baccini, A., Wang, Y., Lauerwald, R., Peng, S., Bastos, A., Cescatti, A., and Yue, C.:
394 Five decades of northern land carbon uptake revealed by the interhemispheric CO₂ gradient, *Nature*, 568, 221–225,
395 <https://doi.org/10.1038/s41586-019-1078-6>, 2019.

396 Cook-Patton, S. C., Leavitt, S. M., Gibbs, D., Harris, N. L., Lister, K., Anderson-Teixeira, K. J., Briggs, R. D.,
397 Chazdon, R. L., Crowther, T. W., and Ellis, P. W.: Mapping carbon accumulation potential from global natural forest
398 regrowth, *Nature*, 585, 545–550, <https://doi.org/10.1038/s41586-020-2686-x>, 2020.

399 Dial, R. J., Beamer, J. P., McDowell, P. D., Herriott, I. C., Milne, B. T., Giardina, C. P., and Sullivan, P. F.: Arctic
400 sea ice retreat fuels boreal forest advance, *Science*, 383, 877–884, <https://doi.org/10.1126/science.adj0832>, 2024.

401 Dial, R. J., Maher, C. T., Hewitt, R. E., and Sullivan, P. F.: Sufficient conditions for rapid range expansion of a boreal
402 conifer, *Nature*, 608, 546–551, <https://doi.org/10.1038/s41586-022-05066-4>, 2022.

403 Dinerstein, E., Olson, D., Joshi, A., Vynne, C., Burgess, N. D., Wikramanayake, E., Hahn, N., Palminteri, S., Hedao,
404 P., and Noss, R.: An ecoregion-based approach to protecting half the terrestrial realm, *BioScience*, 67, 534–545,
405 <https://doi.org/10.1093/biosci/bix014>, 2017.

406 Doerr, S. H., and Santín, C.: Global trends in wildfire and its impacts: perceptions versus realities in a changing world,
407 *Philos. Trans. R. Soc. B Biol. Sci.*, 371, 20150345, <https://doi.org/10.1098/rstb.2015.0345>, 2016.

408 Elmendorf, S. C., Henry, G. H. R., Hollister, R. D., Björk, R. G., Bjorkman, A. D., Callaghan, T. V., and Collier, L.
409 S.: Plot-scale evidence of tundra vegetation change and links to recent summer warming, *Nat. Clim. Change*, 2, 453–
410 457, <https://doi.org/10.1038/nclimate1465>, 2012.

411 [Fan, L., Wigneron, J.-P., Ciais, P., Chave, J., Brandt, M., Sitch, S., Yue, C., Bastos, A., Li, X., Qin, Y., Yuan, W.,](#)
412 [Schepaschenko, D., Mukhortova, L., Li, X., Liu, X., Wang, M., Frappart, F., Xiao, X., Chen, J., ... Fensholt, R.:](#)
413 [Siberian carbon sink reduced by forest disturbances. *Nature Geoscience*, 16\(1\), 56–62.](#)
414 <https://doi.org/10.1038/s41561-022-01087-x>, 2023

415 Forkel, M., Carvalhais, N., Rödenbeck, C., Keeling, R., Heimann, M., Thonicke, K., Reichstein, M., and High-
416 Latitude Ecosystem Modeling Group: Enhanced seasonal CO₂ exchange caused by amplified plant productivity in
417 northern ecosystems, *Science*, 351, 696–699, <https://doi.org/10.1126/science.aac4971>, 2016.

418 Frost, G. V., and Epstein, H. E.: Tall shrub and tree expansion in Siberian tundra ecotones since the 1960s, *Glob.*
419 *Change Biol.*, 20, 1264–1277, <https://doi.org/10.1111/gcb.12406>, 2014.

420 Gauthier, S., Bernier, P., Kuuluvainen, T., Shvidenko, A. Z., and Schepaschenko, D. G.: Boreal forest health and
421 global change, *Science*, 349, 819–822, <https://doi.org/10.1126/science.aaa9092>, 2015.

422 Guay, K. C., Beck, P. S. A., Berner, L. T., Goetz, S. J., Baccini, A., and Buermann, W.: Vegetation productivity
423 patterns at high northern latitudes: a multi-sensor satellite data assessment, *Glob. Change Biol.*, 20, 3147–3158,
424 <https://doi.org/10.1111/gcb.12647>, 2014.

425 Henttonen, H. M., Nöjd, P., and Mäkinen, H.: Environment-induced growth changes in the Finnish forests during
426 1971–2010 – An analysis based on National Forest Inventory, *For. Ecol. Manag.*, 386, 22–36,
427 <https://doi.org/10.1016/j.foreco.2016.12.021>, 2017.

428 Hofgaard, A., Dalen, L., and Hytteborn, H.: Tree recruitment above the treeline and potential for climate-driven
429 treeline change, *J. Veg. Sci.*, 20, 1133–1144, <https://doi.org/10.1111/j.1654-1103.2009.01106.x>, 2009.

430 Holtmeier, F.-K., and Broll, G.: Sensitivity and response of northern hemisphere altitudinal and polar treelines to
431 environmental change at landscape and local scales, *Glob. Ecol. Biogeogr.*, 14, 395–410,
432 <https://doi.org/10.1111/j.1466-822X.2005.00168.x>, 2005.

433 Huang, Y., Crowther, T. W., and Maynard, D. S.: A global map of root biomass across the world’s forests, *Earth Syst.*
434 *Sci. Data*, 13, 4263–4274, <https://doi.org/10.5194/essd-13-4263-2021>, 2021.

435 IPCC: Climate Change ~~2014~~ Synthesis Report, IPCC, Geneva, Switzerland, 2014.

436 IPCC: Global Warming of 1.5°C, IPCC Special Report, 2018.

437 [IPCC: Climate Change Synthesis Report. IPCC, Geneva, Switzerland, 2023.](#)

438 Ju, J., and Masek, J. G.: The vegetation greenness trend in Canada and US Alaska from 1984–2012 Landsat data,
439 Remote Sens. Environ., 176, 1–16, <https://doi.org/10.1016/j.rse.2016.01.001>, 2016.

440 Kajii, Y., Kato, S., Streets, D. G., Tsai, N. Y., Shibata, T., Matsumoto, J., and Kajino, M.: Boreal forest fires in Siberia
441 in 1998: Estimation of area burned and emissions of pollutants by advanced very high resolution radiometer satellite
442 data, J. Geophys. Res. Atmospheres, 107, ACH 4-1–ACH 4-8, <https://doi.org/10.1029/2001JD001078>, 2002.

443 Kharuk, V. I., Ponomarev, E. I., Ivanova, G. A., Dvinskaya, M. L., Coogan, S. C. P., and Flannigan, M. D.: Wildfires
444 in the Siberian taiga, Ambio, <https://doi.org/10.1007/s13280-020-01490-x>, 2021.

445 Koven, C. D.: Boreal carbon loss due to poleward shift in low-carbon ecosystems, Nat. Geosci., 6, 452–456,
446 <https://doi.org/10.1038/ngeo1801>, 2013.

447 Koven, C. D., Hugelius, G., Lawrence, D. M., and Wieder, W. R.: Higher climatological temperature sensitivity of
448 soil carbon in cold than warm climates, Nat. Clim. Change, 7, 817–822, <https://doi.org/10.1038/nclimate3421>, 2017.

449 Krylov, A., McCarty, J. L., Potapov, P., Loboda, T., Tyukavina, A., Turubanova, S., and Hansen, M. C.: Remote
450 sensing estimates of stand-replacement fires in Russia, 2002–2011, Environ. Res. Lett., 9, 105007,
451 <https://doi.org/10.1088/1748-9326/9/10/105007>, 2014.

452 Kuuluvainen, T., and Gauthier, S.: Young and old forest in the boreal: critical stages of ecosystem dynamics and
453 management under global change, For. Ecosyst., 5, 26, <https://doi.org/10.1186/s40663-018-0149-8>, 2018.

454 Liski, J., Perruchoud, D., Karjalainen, T., and Poulton, P.: Increased carbon sink in temperate and boreal forests, Clim.
455 Change, 61, 89–109, <https://doi.org/10.1023/A:1026368803516>, 2003.

456 Mack, M. C., Walker, X. J., Johnstone, J. F., Alexander, H. D., Melvin, A. M., Miller, S. N., and Goetz, S. J.: Carbon
457 loss from boreal forest wildfires offset by increased dominance of deciduous trees, Science, 372, 280–283,
458 <https://doi.org/10.1126/science.abf3903>, 2021.

459 Massey, R., Walker, X. J., Mack, M. C., Johnstone, J. F., Miller, S. N., and Goetz, S. J.: Forest composition change
460 and biophysical climate feedbacks across boreal North America, Nat. Clim. Change, 13, 1368–1375,
461 <https://doi.org/10.1038/s41558-023-01826-4>, 2023.

462 McManus, K. M., Morton, D. C., Masek, J. G., Wang, D., Sexton, J. O., and Nagol, J.: Satellite-based evidence for
463 shrub and graminoid tundra expansion in northern Quebec from 1986 to 2010, Glob. Change Biol., 18, 2313–2323,
464 <https://doi.org/10.1111/j.1365-2486.2012.02708.x>, 2012.

465 Meddens, A. J. H., Hicke, J. A., and Ferguson, C. A.: Spatiotemporal patterns of observed bark beetle-caused tree
466 mortality in British Columbia and the western United States, Ecol. Appl., 22, 1876–1891, <https://doi.org/10.1890/11-1785.1>, 2012.

468 Mekonnen, Z. A., Riley, W. J., Randerson, J. T., Grant, R. F., and Rogers, B. M.: Expansion of high-latitude deciduous
469 forests driven by interactions between climate warming and fire, *Nat. Plants*, 5, 952–958,
470 <https://doi.org/10.1038/s41477-019-0495-6>, 2019.

471 Mollicone, D., Eva, H. D., and Achard, F.: Human role in Russian wildfires, *Nature*, 440, 436–437,
472 <https://doi.org/10.1038/440436a>, 2006.

473 Montesano, P. M., Frost, M., Li, J., Carroll, M., Neigh, C. S. R., Macander, M. J., Sexton, J. O., & Frost, G. V.: A
474 shift in transitional forests of the North American boreal will persist through 2100, *Nature Communications: Earth
475 and Environment*, 5, 1, <https://doi.org/10.1038/s43247-024-01454-z>
476 <https://doi.org/10.1038/s43247-024-01454-z>,
2024.

477 [Montesano, P. M., Neigh, C. S. R., Macander, M. J., Wagner, W., Duncanson, L. I., Wang, P., Sexton, J. O., Miller,
478 C. E., & Armstrong, A. H.: Patterns of regional site index across a North American boreal forest gradient.
479 *Environmental Research Letters*, 18\(7\), 075006. <https://doi.org/10.1088/1748-9326/acdcab>, 2023](#)

480 [Montesano, P. M., Nelson, R., Sun, G., Margolis, H., Kerber, A., & Ranson, K. J.: MODIS tree cover validation for
481 the circumpolar taiga–tundra transition zone. *Remote Sensing of Environment*, 113\(10\), 2130–2141.
482 <https://doi.org/10.1016/j.rse.2009.05.021>, 2009](#)

483 [Montesano, P. M., Sun, G., Dubayah, R. O., & Ranson, K. J.: Spaceborne potential for examining taiga–tundra ecotone
484 form and vulnerability. *Biogeosciences*, 13\(13\), 3847–3861. <https://doi.org/10.5194/bg-13-3847-2016>, 2016](#)

485 Neigh, C. S. R., Tucker, C. J., and Townshend, J. R. G.: North American vegetation dynamics observed with multi-
486 resolution satellite data, *Remote Sens. Environ.*, 112, 1749–1772, <https://doi.org/10.1016/j.rse.2007.08.018>, 2008.

487 Neigh, C. S. R., Nelson, R. F., Ranson, K. J., Margolis, H. A., Montesano, P. M., Sun, G., and Goetz, S. J.: Taking
488 stock of circumboreal forest carbon with ground measurements, airborne and spaceborne LiDAR, *Remote Sens.
489 Environ.*, 137, 274–287, <https://doi.org/10.1016/j.rse.2013.06.019>, 2013.

490 Neigh, C., Montesano, P. M., Sexton, J. O., Wooten, M., Wagner, W., Feng, M., Carvalhais, N., Calle, L., & Carroll,
491 M. L.: Russian forests show strong potential for young forest growth, *Nature Communications: Earth and
492 Environment*, 6, 1, <https://doi.org/10.1038/s43247-025-02006-9>, 2025.

493 Norby, R. J., and Zak, D. R.: Ecological lessons from Free-Air CO₂ Enrichment (FACE) experiments, *Annu. Rev.
494 Ecol. Evol. Syst.*, 42, 181–203, <https://doi.org/10.1146/annurev-ecolsys-102209-144647>, 2011.

495 Odum, E. P.: The strategy of ecosystem development, *Science*, 164, 262–270,
496 <https://doi.org/10.1126/science.164.3877.262>, 1969.

497 Pan, Y., Birdsey, R. A., Fang, J., Houghton, R., Kauppi, P. E., Kurz, W. A., and Phillips, O. L.: A large and persistent
498 carbon sink in the world’s forests, *Science*, 333, 988–993, <https://doi.org/10.1126/science.1201609>, 2011.

499 [Pan, Y., Birdsey, R. A., Phillips, O. L., Houghton, R. A., Fang, J., Kauppi, P. E., Keith, H., Kurz, W. A., Ito, A.,
500 Lewis, S. L., Nabuurs, G.-J., Shvidenko, A., Hashimoto, S., Lerink, B., Schepaschenko, D., Castanho, A., &](#)

501 [Murdiyarso, D.: The enduring world forest carbon sink. *Nature*, 631\(8021\), 563–569. \[https://doi.org/10.1038/s41586-\]\(https://doi.org/10.1038/s41586-024-07602-x\)](https://doi.org/10.1038/s41586-024-07602-x)
502 [024-07602-x](https://doi.org/10.1038/s41586-024-07602-x), 2024

503 Piao, S., Wang, X., Ciais, P., Zhu, B., Wang, T., and Liu, J.: Characteristics, drivers and feedbacks of global greening,
504 *Nat. Rev. Earth Environ.*, 1, 14–27, <https://doi.org/10.1038/s43017-019-0001-x>, 2020.

505 Randerson, J. T., Liu, H., Flanner, M. G., Chambers, S. D., Jin, Y., Hess, P. G., and Rasch, P. J.: The impact of boreal
506 forest fire on climate warming, *Science*, 314, 1130–1132, <https://doi.org/10.1126/science.1132075>, 2006.

507 Rees, W. G., Stammer, F. M., Danks, F. S., and Vitebsky, P.: Is subarctic forest advance able to keep pace with
508 climate change?, *Glob. Change Biol.*, 26, 3965–3977, <https://doi.org/10.1111/gcb.15181>, 2020.

509 Rotbarth, R., Walker, X. J., Mack, M. C., Goetz, S. J., Johnstone, J. F., and Miller, S. N.: Northern expansion is not
510 compensating for southern declines in North American boreal forests, *Nature Communications*, 14, 3373,
511 <https://doi.org/10.1038/s41467-023-39128-8>, 2023.

512 Sato, H., Kobayashi, H., Iwahana, G., and Ohta, T.: Endurance of larch forest ecosystems in eastern Siberia under
513 warming trends, *Ecol. Evol.*, 6, 5690–5704, <https://doi.org/10.1002/ece3.2264>, 2016.

514 Scheffer, M., Hirota, M., Holmgren, M., van Nes, E. H., and Chapin, F. S.: Thresholds for boreal biome transitions,
515 *Proc. Natl. Acad. Sci. USA*, 109, 21384–21389, <https://doi.org/10.1073/pnas.1219844110>, 2012.

516 Schuur, E. A. G., Abbott, B. W., Bowden, W. B., Brovkin, V., Camill, P., Davidson, E. A., and Hayes, D. J.: Climate
517 change and the permafrost carbon feedback, *Nature*, 520, 171–179, <https://doi.org/10.1038/nature14338>, 2015.

518 Sexton, J. O., Noojipady, P., Song, X.-P., Feng, M., Song, D. X., Kim, D. H., and Hansen, M. C.: Global, 30-m
519 resolution continuous fields of tree cover: Landsat-based rescaling of MODIS vegetation continuous fields with
520 LiDAR-based estimates of error, *Int. J. Digit. Earth*, 6, 427–448, <https://doi.org/10.1080/17538947.2013.786146>,
521 2013.

522 Walker, X. J., Rogers, B. M., Baltzer, J. L., Baltzer, B., Barrett, M., Bourgeau-Chavez, L., and Mack, M. C.: Increasing
523 wildfires threaten historic carbon sink of boreal forest soils, *Nature*, 572, 520–523, [https://doi.org/10.1038/s41586-](https://doi.org/10.1038/s41586-019-1474-y)
524 [019-1474-y](https://doi.org/10.1038/s41586-019-1474-y), 2019.

525 UNFCCC: Report of the Conference of the Parties on its Seventh Session, held at Marrakesh from 29 October to 10
526 November 2001, Addendum Part Two, United Nations Framework Convention on Climate Change, 2002

527 Xi, Y., Zhang, W., Wei, F., Fang, Z., & Fensholt, R.: Boreal tree species diversity increases with global warming but
528 is reversed by extremes, *Nature Plants*, <https://doi.org/10.1038/s41477-024-01794-w>, 2024.

529 Yan, Y., Piao, S., Hammond, W. M., Chen, A., Hong, S., Xu, H., Munson, S. M., Myneni, R. B., & Allen, C. D.:
530 Climate-induced tree-mortality pulses are obscured by broad-scale and long-term greening, *Nature Ecology and*
531 *Evolution*, <https://doi.org/10.1038/s41559-024-02372-1>, 2024.

532 Zhu, Z., Piao, S., Myneni, R. B., Huang, M., Zeng, Z., Canadell, J. G., and Ciais, P.: Greening of the Earth and its
533 drivers, *Nat. Clim. Change*, 6, 791–795, <https://doi.org/10.1038/nclimate3004>, 2016.

